ALTERNATIVE WAYS OF MODELLING STABILISED EXCAVATIONS

Sinem Bozkurt[1*], Ayman Abed[1], and Minna Karstunen[1]

KEYWORDS

deep mixing, deep excavations, volume averaging, soft clay, lime-cement columns

ABSTRACT

The realistic estimation of the soft clay response in deep excavations stabilised with lime-cement columns highly relies on the consideration of nonlinear elastoplastic soil behaviour and three-dimensional (3D) effects. In this paper, deep-mix columns were simulated using both linear elastic and nonlinear elastoplastic constitutive models to illustrate their influence on the deformations of the sheet-pile wall. Model parameters were calibrated using high-quality laboratory tests conducted on both field-mix and laboratory-mix samples. Subsequently, the inherent 3D nature of stabilised soft clay was incorporated into a plane strain analysis using a volume averaging technique. The technique, implemented for 2D analysis, accommodates the use of different advanced soil models to represent the stabilised clay, consisting of the soft clay and columns. The results indicate that relying solely on one-dimensional compression tests when modelling stabilised clay leads to an underestimation of the deformations and structural forces of the sheet-pile wall. The proposed technique maps the actual 3D problem into an equivalent 2D, thus holding the potential to efficiently capture real soil behaviour.

1. INTRODUCTION

Deep mixing using lime and/or cement as a cementitious binder has been used over 50 years simultaneously in Japan and Scandinavian countries to improve the strength and compressibility of soft soils. In Nordic countries the dry soil mixing method (DSM) is widely accepted solution in stabilising soft clay (e.g. [1-3]). Additionally, there are applications for sandy soils with insufficient natural water content for proper hydration of the binder using the wet or modified dry mixing methods (i.e. [4, 5]).

[1] Chalmers University of Technology, Department of Architecture and Civil Engineering, Gothenburg, SE-412 96, Sweden
[*] sinem.bozkurt@chalmers.se

The hydromechanical response of the stabilised clay when mixed with stabilising agents differs from the natural or reconstituted states. To simulate the response of artificially cemented clays, traditionally, simple elastic perfectly plastic soil models like Mohr-Coulomb are widely adopted, despite its limitations in realistically representing soil behaviour, such as the absence of hardening/softening plasticity and stress-dependent stiffness. Current guidelines (e.g. [6-9]) for deep mixing design typically propose rigid-plastic solutions and the weighted strength/stiffness based on [10, 11], primarily tailored for embankment applications. These guidelines establish empirical links between the undrained shear strength (determined via vane, unconfined compressive strength (UCS), fall-cone, static penetration tests (FKPS/ FOPS), etc.) and the stiffness. In stabilised excavations with deep mixing, especially in urban settings where serviceability governs the design, stress-dependant stiffness and the influence of the soft clay on the overall response becomes equally critical.

In this paper, a braced excavation stabilised with lime-cement (LC) columns using DSM was investigated by adopting both linear elastic and nonlinear elastoplastic soil models for plane strain (2D) fully coupled consolidation analyses. In the analyses, the stabilised material in the passive side of the excavation was first simulated based on current practice by using averaged strength and stiffness. Later, a three-dimensional (3D) analysis was performed to account for the hydromechanical response of both the soft clay and LC columns separately. Finally, to take into account 3D effects and the different response of individual materials, a volume averaging technique was implemented into a 2D finite element code. The response of the homogenised material involving the soft clay and columns was described based on the 3D simulation. The lateral deformation profile and maximum moment of the sheet-pile wall (SPW) were compared among the alternative methods.

2. NUMERICAL MODELLING

The numerical analyses were performed based on a five-meter-deep braced excavation for an arbitrary consolidation period taking into account transient flow. LC column construction in the excavated region was assumed to be wished-in-place, and therefore no installation effects during and after the deep mixing were considered. These effects can be incorporated into simulation through an external strain/load application if field instrumentation data exist (i.e. [12]). The excavation was supported by a fifteen-meter-long SPW and single row of struts with a five-meter spacing in the out-of-plane axis. LC columns, each with a diameter of 0.7 m and a length of 10 m, were arranged in a square grid pattern with a spacing of 2.5 m and a 20 cm overlap, as illustrated in Figure 1(a).

The 2D analyses consisted of utilising simple averaging of stiffness/strength with a linear or nonlinear soil model. In contrast, in the 3D simulation, the col-

umns and soft clay were simulated separately using different nonlinear elasto-plastic soil models to include the varied soil responses (i.e. stress/strain) in a homogenised material (i.e. stabilised clay) (refer to Figure 1(b)). In the 3D case, the overlapping column grid was simplified into a rectangular form for the sake of simplicity, as the primary focus is not on optimising 3D analysis but rather on assessing the influence of the individual constituents on the deformation profile and the structural forces of the SPW. Additionally, to describe the hydromechanical response of the homogenised material, a volume averaging technique (VAT), elaborated in Section 3, was adopted for 2D analysis.

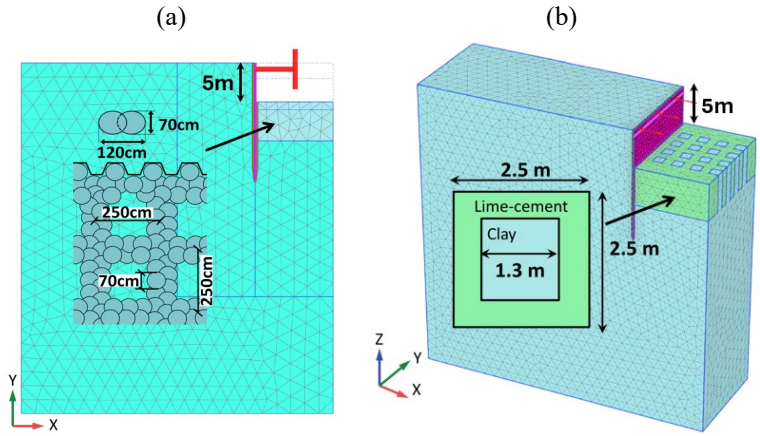

Figure 1. The used FE model in (a) 2D and (b) 3D analyses.

To reduce the effect of discretisation, comparable meshes were utilised in the 2D analyses with 1,125 15-node triangular elements totalling 9276 nodes, whilst in the 3D simulation, 42,294 10-node tetrahedral elements totalling 67,835 nodes were employed. The discretised geometry in the 2D and 3D simulations (PLAXIS 2D & 3D, version 23) at the final excavation phase are presented in Figure 1.

2.1. Modelling soft clay

The hydromechanical response of the soft clay was represented by the S-CLAY1S model [13]. The model accounts for the initial anisotropy, the evolution in fabric and in interparticle bonding of natural soft clays owing to plastic straining. The plastic straining governs the progressive loss of bonding (χ) and the volumetric component changes in the size of the intrinsic yield surface. The isotropic preconsolidation pressure (p'_m) defines the size of the natural yield surface. p'_m is linked with the size of the imaginary intrinsic surface where all bonding is destroyed ($p'_m = (1+\chi)p'_{mi}$). Both the yield and the intrinsic surfaces have the same orientation.

To ensure a more realistic simulation, model parameters for soft clay were taken from a West Link railway tunnel construction project, underneath the centre of Gothenburg, based on a previous study [12]. The hydraulic conductivity of the stabilised clay and natural clay were assumed to be of the same order (0.75×10^{-4} m/day). The model parameters, computed from several CAUE/CADE (anisotropically consolidated undrained/drained triaxial tests in extension) and IL (incrementally loaded oedometer) tests performed on the field samples, are shown in Table 1.

Table 1. S-CLAY1S parameters for the soft clay.

Definition	Value [-]
$\boldsymbol{\lambda_i}$, intrinsic compression index	0.2
$\boldsymbol{\kappa}$, swelling index	0.02
$\boldsymbol{\upsilon'}$, Poisson's ratio	0.2
M, critical state stress ratio	1.10
$\boldsymbol{\mu}$, absolute effectiveness of rotational hardening	50
$\boldsymbol{\beta}$, relative effectiveness of rotational hardening	0.64
a, absolute rate of destructuration due to volumetric strain	12
b, relative rate of destructuration due to shear strain	0.4
$\boldsymbol{\chi_0}$, initial amount of bonding	6
$\boldsymbol{\alpha_0}$, initial anisotropy	0.42
OCR, overconsolidation ratio	1.20
$\mathbf{K_0}$, coefficient of earth pressure at rest	0.54
$\mathbf{e_0}$, initial void ratio	1.90

2.2. Modelling deep-mix columns

The deep-mix columns were modelled using the Matsuoka-Nakai hardening (MNhard) [14] and Mohr Coulomb (MC) soil models. The MNhard model employs hyperbolic stress-strain relationship for shear hardening and the ultimate failure is computed based on the Matsuoka-Nakai failure criterion [15]. During the stages of primary loading (secant modulus, E'_{50}) and unloading-reloading (un-/reloading modulus, E'_{ur}), stress-dependent moduli can be computed with a power law using Equation (1).

$$E'_{50,ur} = E'^{ref}_{50,ur} \left(\frac{\sigma'_3 + c' \cot\phi'}{\sigma'^{ref} + c' \cot\phi'} \right)^m \quad (1)$$

where m defines the amount of stress dependency and controls the shape of the yield surface. Shear modulus can be estimated using elasticity theory ($G=E'/(1+\upsilon')$) and can be simulated using triaxial test data.

The Matsuoka-Nakai failure criterion is determined by the average of the mobilised planes (SPM) in 3D effective stress space using Equation (2), while the MC failure is defined by shear (τ) and normal (σ) effective stresses considering major and minor principal stresses on the failure plane with Equation (3). As demonstrated in Section 4, for serviceability limit states neither failure criterion nor strength (c' and ϕ') are influential.

$$\frac{\tau_{SMP}}{\sigma_{SMP}} = \frac{2}{3}\sqrt{\frac{(\sigma_1-\sigma_2)^2}{4\sigma_1\sigma_2} + \frac{(\sigma_2-\sigma_3)^2}{4\sigma_2\sigma_3} + \frac{(\sigma_3-\sigma_1)^2}{4\sigma_3\sigma_1}} \tag{2}$$

$$\tau_f = c' + \sigma'_f \tan\phi' \tag{3}$$

The parameters for the MC model parameters were computed using the unconfined compression strength (UCS) from data provided by [16]. The tests performed on field-mixed samples, taken from various depths for the West Link project, are presented in Figure 2. The proportion of binder was 50% lime and 50% cement with 80 kg/m^3 by dry weight.

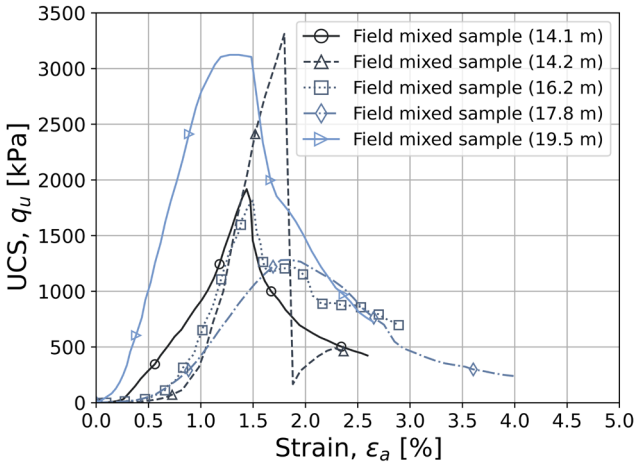

Figure 2. UCS tests performed on field mixed samples (adopted from [16]).

According to Figure 2, although the available samples were selected to be able to conduct the unconfined compression tests (UCT), possible low-strength regions along the stabilised zone are likely to affect overall response, as the available samples may not fully represent the LC columns. The significant variation of the unconfined strength, q_u, is noteworthy, with a coefficient of variation of

46%. The minimum, maximum and average values of q_u are 1.3-3.3 and 2.3 MPa, respectively. The average E'_{50} was computed as 216 MPa from the laboratory data, which corresponded to 230 MPa using the lower bound estimation of E'_{50}/q_u defined as 100 in [9]. Considering the large variation in measured q_u, the upper and lower boundaries were investigated for the 2D simulations using the simple stiffness averaging method.

To explore the influence of the strength, the lower boundary was determined by averaging the effective strength parameters of the column and *in situ* clay, while the upper boundary values belong to the LC columns calculated from triaxial tests. Effective strength parameters are derived from triaxial tests. The averaged stabilised clay properties using the MC model are presented in Table 2.

Table 2. The averaged MC soil model parameters for stabilised region (2D FEA).

	γ_n (kN/m^3)	E_{50} (kPa)	ϕ' (°)	c' (kPa)	υ' (-)
Lower, $q_{u(min)}$	16.5	97500	35	15	0.25
Upper, $q_{u(avg)}$	16.5	171220	37	20	

The parameters for the MNhard model for the stabilised clay were determined and calibrated using a series of CAUE and IL tests performed on both *in situ* mixed and laboratory mixed samples [11]. In this study, for the 2D finite element analysis (FEA), a simple stiffness/strength averaging technique was initially applied, using a simplified area replacement ratio of 0.73 ($a_r = (2.5^2 - 1.3^2) / 2.5^2$), based on the overlapping column square-grid (see Figure 1(a) and Table 3). The average stiffness of the stabilised clay was computed using the arithmetic mean of the soft clay (E'_{50}=15MPa, E'_{ur}=39MPa) and LC column (E'_{50}=85MPa, E'_{ur}=180MPa) stiffness. In contrast, in the 3D analysis and in the subsequent 2D analysis with VAT, LC columns were represented without the averaging by using the values presented in Table 4.

Table 3. The averaged MNhard soil model parameters for stabilised region (2D FEA).

γ_n (kN/m^3)	G_{50}^{ref} (kPa)	G_{ur}^{ref} (kPa)	p^{ref} (kPa)	m (-)	ϕ' (°)	c' (kPa)	υ' (-)
16.5	25000	56000	100	0.65	37	20	0.25

Table 4. MNhard soil model parameters for the columns (2D VAT and 3D FEA).

γ_n (kN/m^3)	G_{50}^{ref} (kPa)	G_{ur}^{ref} (kPa)	p^{ref} (kPa)	m (-)	ϕ' (°)	c' (kPa)	υ' (-)
16.5	28000	75000	100	0.65	37	20	0.25

3. VOLUME AVERAGING TECHNIQUE

The volume averaging technique (VAT) has been used to describe the response of the composite materials consisting of two or more materials [17]. The method has been employed to simulate settlements in soft clay underneath the road embankments stabilised with deep mixed/stone columns [18, 19]. The stress-strain increments within the composite material can be calculated by averaging the increments of the individual constituents, under the assumption of an equivalent homogenised material. The averaging rules that form the basis for describing the response of the equivalent material are given in Equations (4) and (5).

$$\Delta\boldsymbol{\sigma}^{\boldsymbol{eq}} = \Omega_s \Delta\boldsymbol{\sigma}^{\boldsymbol{s}} + \Omega_c \Delta\boldsymbol{\sigma}^{\boldsymbol{c}} \tag{4}$$

$$\Delta\boldsymbol{\varepsilon}^{\mathbf{eq}} = \Omega_{\mathrm{s}} \Delta\boldsymbol{\varepsilon}^{\mathbf{s}} + \Omega_{\mathrm{c}} \Delta\boldsymbol{\varepsilon}^{\mathbf{c}} \tag{5}$$

where Ω represents the fraction of individual materials, while $\Delta\boldsymbol{\sigma}$ and $\Delta\boldsymbol{\varepsilon}$ stand for the increments of stress and strain tensors, respectively. The subscripts *c*, *s* and superscript *eq* denote the columns, soft clay and equivalent material. Ω can be computed considering the representative plan area of the constituents for evenly distributed columns. Alternatively, the geometry can be divided into subsections to increase the accuracy of the calculations.

VAT has not been applied to stabilised excavation problems owing to difficulties in assessing interaction mechanism between the soft clay and deep-mix columns. In this study, the stress-strain distribution of the equivalent material, comprising the natural clay and deep-mix columns, was generalised based on the 3D analysis by investigating the relevant equilibrium and kinematics conditions. The fundamental considerations to preserve local equilibrium are presented in Equations (6)-(8). In the equations, global coordinate system for plain strain analysis was utilised where x and z designate the horizontal axes, and y is the vertical axis.

$$\Delta\sigma'^{\mathrm{eq}}_{\mathrm{zz}} = \Delta\sigma'^{\mathrm{c}}_{\mathrm{zz}} = \Delta\sigma'^{\mathrm{s}}_{\mathrm{zz}} \tag{6}$$

$$\Delta\tau^{\mathrm{eq}}_{\mathrm{yz}} = \Delta\tau^{\mathrm{c}}_{\mathrm{yz}} = \Delta\tau^{\mathrm{s}}_{\mathrm{yz}} \tag{7}$$

$$\Delta\tau^{\mathrm{eq}}_{\mathrm{zx}} = \Delta\tau^{\mathrm{c}}_{\mathrm{zx}} = \Delta\tau^{\mathrm{s}}_{\mathrm{zx}} \tag{8}$$

Similarly, compatibility in kinematics of the strain field is maintained using Equations (9)-(11).

$$\Delta\varepsilon_{xx}^{eq} = \Delta\varepsilon_{xx}^{c} = \Delta\varepsilon_{xx}^{s} \quad (9)$$

$$\Delta\varepsilon_{yy}^{eq} = \Delta\varepsilon_{yy}^{c} = \Delta\varepsilon_{yy}^{s} \quad (10)$$

$$\Delta\gamma_{xy}^{eq} = \Delta\gamma_{xy}^{c} = \Delta\gamma_{xy}^{s} \quad (11)$$

The elastic stiffness matrix of the equivalent material ($\mathbf{D^{eq}}$) is constituted using the stress equality conditions that results in an independent strain distribution within the soft clay and columns. The independent strain distribution can be formed analytically through the strain redistribution matrices, $\mathbf{S_1^{s,c}}$ using continuity constrains (Equations (9)-(11)). Thereby, the stress increments in the equivalent material can be expressed in terms of effective stresses of the individual materials using Equations (4) and (12), and $\mathbf{D^{eq}}$ can be established, provided that the elastic stiffness matrix of the individual materials, $\mathbf{D^{s,c}}$, are known (Equation (13)).

$$\mathbf{\Delta D^{eq}\varepsilon^{eq}} = \Omega_s \mathbf{D^s S_1^s \varepsilon^{eq}} + \Omega_c \mathbf{D^c S_1^c \varepsilon^{eq}} \quad (12)$$

$$\mathbf{D^{eq}} = \Omega_s \mathbf{D^s S_1^s} + \Omega_c \mathbf{D^c S_1^c} \quad (13)$$

VAT was implemented into the commercial finite element code Plaxis2D (version 23) as a user-defined soil model (UDSM). Local integration was achieved using an implicit scheme to solve nonlinear equations iteratively. During the iterative calculations, if the equilibrium constraint is not achieved, stress states revert to previous values and strain increments are redistributed between the constituents, initiated by the return mapping scheme. The technique therefore always satisfies both the local balance and maintains the continuity of kinematics.

4. RESULTS

The stress-strain response of the braced excavation stabilised with LC columns was initially investigated following the current design guidelines. The investigation involved using the average stiffness/strength of the clay and column materials. In the simulations, both linear and nonlinear elastoplastic constitutive models were utilised to model the stabilised clay in the passive side of the excavation. Either the MC or MNhard model was employed, incorporating the averaged stiffness and strength parameters as indicated in Table 2 and 3. The natural soil, the soft clay, was represented by the anisotropic S-CLAY1S model. However, the adopted simple stiffness/strength averaging approach unfortunately does not account for the hydromechanical response of the soft clay.

The results of the simulations were compared to evaluate the effects of choosing between linear and nonlinear model options, as depicted in Figure 3. When calculating the average stiffness using the MC model, the stiffness of the columns was determined, taking into consideration the variability of q_u. Consequently, both the minimum and average values were investigated. The stiffness calculated from the average strength (q_{uavg}) led to a significantly lower maximum lateral deformation of approximately 3 mm, along the first 5 meters of the excavation. In contrast, using the minimum strength (q_{umin}) resulted in approximately 5 mm (see Figure 3(b)). Employing the MNhard model yielded a maximum lateral deformation of 9 mm. Evidently, regardless of the model choice, averaging the strength appears to have no effect on the lateral deformation profile of the SPW, as it is governed by the serviceability limit state. This is particularly relevant for braced excavations in urban areas, where the excavations are designed for restricted lateral deformations. In Figure 3(a), the lateral deformation profile was affected by the averaged strength only marginally. The difference arises from the formulation of the MNhard model in which the stress dependent stiffness is a function of the strength parameters (c' and ϕ') outlined in Equation (1).

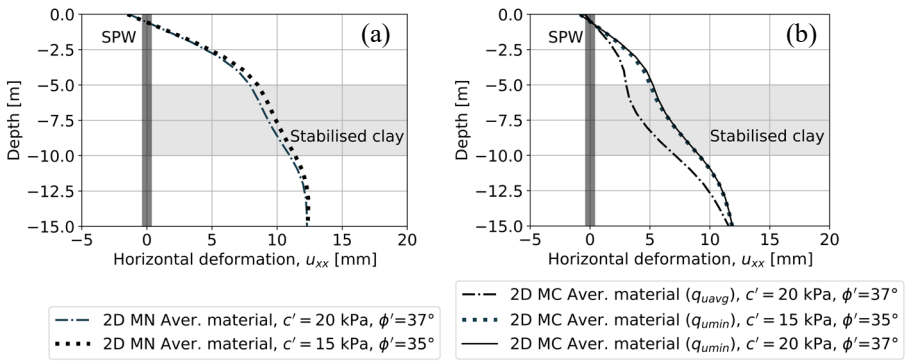

Figure 3. Lateral pile deformation profile at the final excavation stage with/without averaging strength. (a) MNhard model and (b) MC model.

To take into account the hydromechanical response of the soft clay, the braced excavation was investigated using a 3D analysis. The distinct mechanical properties of the natural clay and columns were simulated using different advanced constitutive models (S-CLAY1S and MNhard models, respectively) with conventional separate soil clusters (Figure 1(b)). Subsequently, the stress-strain response of the individual materials identified in the 3D simulation was incorporated into 2D analysis using VAT elaborated in Section 3.

The results of the numerical simulations on the lateral deformation profile and moment distribution of the SPW, using the alternative methods with different constitutive model choices, were compared in Figure 4 and 5.

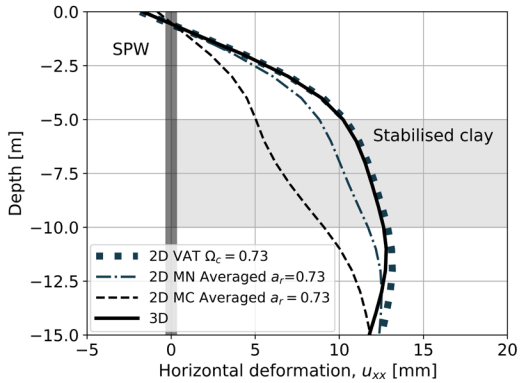

Figure 4. SPW lateral deformation profile at the final excavation stage for alternative methods.

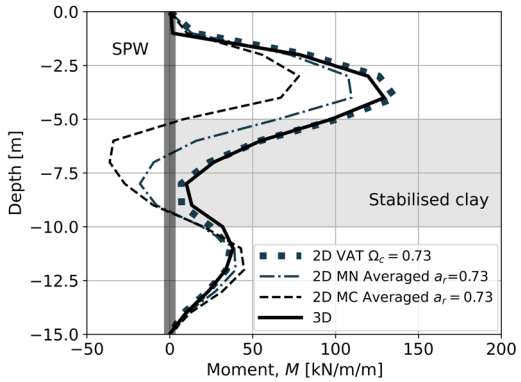

Figure 5. SPW moment profile at the final excavation stage for alternative methods.

The choice of the linear elastic perfectly plastic MC model led to an underestimation of the lateral deformations as well as the maximum moment of the SPW (see Figures 4 and 5). Employing a hardening/softening plasticity model (i.e. MNhard) resulted in a deformation and moment profile more closely aligned with the 3D simulation. Nevertheless, the closest representation of the deformation profile in the 3D simulation was achieved by incorporating the soft clay response using VAT in a plane strain simulation. The results of the 2D simulation with VAT demonstrate robust agreement with those obtained from the 3D simulation.

5. CONCLUSIONS

2D and 3D fully coupled numerical analyses of a braced excavation stabilised with LC were performed. Initially, the stabilised clay in the passive side of the excavation was simulated using the averaged strength and stiffness based on current practice by adopting both linear elastic perfectly plastic and nonlinear elastoplastic soil models for the 2D analyses. The results highlight the inadequacy of one-dimensional compression tests (UCT) for modelling stabilised soft clay, which leads to underestimation of deformations and structural forces.

Subsequently, a separate 3D analysis was performed to address the hydromechanical response of the soft clay and LC columns individually. To account for the 3D nature of deep excavations stabilised with deep-mix columns and the distinct response of the clay and columns, a volume averaging technique (VAT) was integrated into a 2D finite element code. The proposed VAT is a computationally efficient tool, with the potential to capture real soil behaviour with high fidelity. Using soil models that employ hardening/softening plasticity and/or stress-dependent stiffness led to a more accurate representation of the stabilised clay, accounting for the response of both the deep-mix columns and soft clay.

ACKNOWLEDGEMENT

The work is funded by Formas (Research Council for sustainable Development) and Swedish Transport Administration via BIG (Better Interaction in Geotechnics). The work is done as part of Digital Twin Cities Centre that is supported by Sweden's Innovation Agency VINNOVA.

REFERENCES

[1] H. Löfroth: Properties of 10-year-old lime-cement columns. Deep mixing 5, 2005.

[2] R. Ignat, S. Baker, M. Karstunen, S. Liedberg, & S. Larsson: Numerical analyses of an experimental excavation supported by panels of lime-cement columns. Comput. Geotech. 118, 103296, 2020.

[3] S. Larsson: The Nordic dry deep mixing method: Best practice and lessons learned. In Deep Mixing-An Online Conference (pp. 30-p). DFI Deep Foundation Institute, 2021.

[4] J. Gunther, G. Holm, G. Westberg, & H. Eriksson: Modified Dry Mixing (MDM) – A New Possibility in Deep Mixing. In Geotechnical Engineering for Transportation Projects, 2004.

[5] S. Hov, P. Paniagua, C. Sætre, H. Rueslåtten, I. Størdal, M. Mengede, & C. Mevik: Lime-cement stabilisation of Trondheim clays and its impact on carbon dioxide emissions. Soils and Foundations, 62(3), 101162, 2022.

[6] EuroSoilStab: Development of design and construction methods to stabilize soft organic soils: Design guide for soft soil stabilization. *CT97-0351, European Commission, Industrial and Materials Technologies Programme (Rite-EuRam III) Bryssel*, 2002.

[7] EN14679: European Standard, Execution of Special Geotechnical Works – Deep Mixing, 2005.

[8] TK GEO: Technical requirements for geotechnical constructions. Publication 2013:0667, Swedish Transportation Administration, Borlänge. In Swedish, 2013.

[9] SGF: Lime and lime cement columns - Guide for project planning, construction and inspection. SGF Report 2:2000, Swedish Geotechnical Society. In Swedish, 2000.

[10] B. B. Broms, & P. Boman: Lime Columns—A New Foundation Method. Journal of the Geotechnical Engineering Division, 105(4), 539–556, 1979.

[11] B. B. Broms: Lime and lime/cement columns. Ground Improvement, 2, 252–330, 2004.

[12] S. Bozkurt, A. Abed, & M. Karstunen: Finite element analysis for a deep excavation in soft clay supported by lime-cement columns. Computers and Geotechnics, 162, 105687, 2023.

[13] M. Karstunen, H. Krenn, S. J. Wheeler, M. Koskinen, & R. Zentar, Effect of Anisotropy and Destructuration on the Behavior of Murro Test Embankment. International Journal of Geomechanics, 5(2), 87–97, 2005.

[14] T. Benz: Small-Strain Stiffness of Soils and its Numerical Consequences. PhD thesis, University of Stuttgart, Germany, 2007.

[15] H. Matsuoka, & T. Nakai: Stress-deformation and strength characteristics of Soil Under Three Different Principal Stresses. Proceedings of the Japan Society of Civil Engineers, 1974, Volume 1974, Issue 232, 59-70, 1974.

[16] Swedish Transport Administration: Fullskaleförsök DDM (Dry Deep Mixing) i passivzon, delprojekt E02 Centralen, Västlänken. Technical report. TRV 2015/74805. Swedish Transport Administration, 2018.

[17] Z. Hashin: Analysis of Composite Materials—A Survey. Journal of Applied Mechanics 50, 481–505, 1983.

[18] H. F. Schweiger, & G. N. Pande: Numerical analysis of stone column supported foundations. Computers and Geotechnics, 2(6), 347–372, 1986.

[19] U. Vogler: Numerical modelling of deep mixing with volume averaging technique. PhD thesis, The University of Strathclyde, 2009.